PAPER • OPEN ACCESS

Simulation to fabrication—understanding the effect of NiAuCu alloy catalysts for controlled growth of graphene at reduced temperature

To cite this article: Huahan Zhan et al 2019 Mater. Res. Express 7 015603

View the article online for updates and enhancements.

Recent citations

Low-temperature chemical vapor deposition growth of graphene films enabled by ultrathin alloy catalysts Samuel Olson et al



IOP ebooks™

Bringing together innovative digital publishing with leading authors from the global scientific community.

Start exploring the collection-download the first chapter of every title for free.

Materials Research Express



OPEN ACCESS

RECEIVED

4 October 2019

REVISED

27 October 2019

ACCEPTED FOR PUBLICATION 26 November 2019

PURIISHED

9 December 2019

Original content from this work may be used under the terms of the Creative Commons Attribution 3.0 licence.

Any further distribution of this work must maintain attribution to the author(s) and the title of the work, journal citation and DOI.



PAPER

Simulation to fabrication—understanding the effect of NiAuCu alloy catalysts for controlled growth of graphene at reduced temperature

Huahan Zhan^{1,3}, Bin Jiang², Otto Zietz¹, Samuel Olson¹ and Jun Jiao¹

- ¹ Department of Mechanical and Materials Engineering, Portland State University, 97201, OR, United States of America
- ² Fariborz Maseeh Department of Mathematics and Statistics, Portland State University, 97201, OR, United States of America
- Department of Physics, Xiamen University, 361005, People's Republic of China

-mail: jiaoj@pdx.edu

Keywords: graphene, NiAuCu alloy catalyst, chemical vapour deposition, low temperature, density function theory

Abstract

It is a significant challenge to grow large-scale, high quality, monolayer graphene at low temperature for the applications in industry, especially for the complementary metal oxide semiconductor fabrication process. To overcome this difficulty, we simulated the decomposition of acetylene (C_2H_2) on (100) surfaces of primarily nickel (Ni) catalysts with small mol fractions of gold (Au) and copper (Cu), using a 4 \times 4 \times 4 periodic supercell model. Based on the calculation of the reaction energies to decompose the C-H or C \equiv C bonds on different catalyst surfaces, a differential energy is proposed to clearly scale the decomposition difficulties such that larger differential energy leads to easier control of the monolayer growth. It is observed that on the NiAuCu alloy surface with a mol fraction 0.0313 of both Au and Cu, the differential energy of the C-H bonds and the C \equiv C bond are both positive, showing an obvious modulation effect on the decomposition of C_2H_2 and the catalytic activites. The simulation result is consistent with the growth of uniform monolayer graphene on silicon dioxide substrate at 500°C by plasma enhanced chemical vapor deposition with C_2H_2 precursor and Ni alloy catalysts with 1 wt% Au and 1 wt% Cu.

1. Introduction

The distinct properties of graphene make it one of the most promising materials for immense applications in optoelectronic devices, biochemical and biomedical sensors [1–4]. For the applications in industry, especially for the complementary metal oxide semiconductor (CMOS) fabrication process, large-scale, high quality, low temperature grown graphene is essential. However, there still remains a significant challenge in graphene layer number control at reduced temperature [5–7]. Recently, plasma-enhanced chemical vapor deposition (PECVD) has been intensively employed in the growth of high-quality graphene with different types of catalysts [8, 9]. Many strategies have been taken by adopting different methodologies in the modulation of plasma, precursors, substrates, and catalysts, etc [7, 10–12]. To understand the growth mechanism and kinetics of the experimental growth of graphene by CVD, theoretical simulations have also been widely carried out, and the first principle calculation, density function theory, Monte Carlo, and molecular dynamics are the most popular methods [13–17].

The PECVD growth of graphene on silicon dioxide substrate, using transition metals such as Ni, Cu or related alloys like NiAu, NiCu, and AuCu as catalysts has been explored in recent years, with distinct growth behaviors observed [6, 18–22]. For example, it is easier to grow multiple layer graphene on Ni surface at low temperature, and the graphene domains are in polygonal shapes with straight edges and sharp vertices. It is easier to grow monolayer graphene on Cu surface, however at rather high temperature, usually presenting with a diffusion-dominated growth behavior, and the graphene domains are often in flower shaped flakes [6, 15, 16, 23, 24]. What cause such different growth behavior?

The decomposition of carbon precursors is another critical issue that plays an import role for the CVD process. The different products of decomposition have a great impact on the behavior of graphene domain

formation, affecting growth rate, layer thickness, defects, and morphology of overall graphene. This suggests it is possible to optimize the growth by understanding the transition metals and their bimetallic or their alloys in relation to the plasma power for the ionization of the carbon precursors. Also, the adsorption on different surfaces often varies depending on different lattice faces and different catalysts. For example, using CH4 as a precursor on Ni surfaces, the decomposition mainly leads to atomic carbon [25, 26]. That is, CH₄ is easier to be decomposed completely. While on the Cu surfaces, the partially dehydrogenated species, such as CH_i (i = 1, 2,3), are the dominant products, i.e., CH_4 is usually decomposed incompletely [25, 27]. Moreover, the decomposition of CH₄ on Ni(100) surface is more active than that of on (111) surface but less active than that of on (110) surface [16]. Recently, Woo et al has grown uniform monolayer graphene on a metal thin film over silicon substrate at 600 °C, by inductively coupled plasma enhanced chemical vapor deposition (ICPCVD), using acetylene (C_2H_2) as the carbon precursor, and bimetallic catalyst such as $Cu_{1-x}Ni_x$ and $Au_{1-x}Ni_x$, in which the catalytic reaction was controlled on the metal surface [15]. Here x is the weight composition of Ni in the alloy, and x < 0.2. In other words, bulk Cu or bulk Au was used as primary catalyst. It was observed that addition of Ni to the bulk Cu catalyst enabled synthesis temperature reduction due to the increased catalytic activity of Ni compared to Cu. However, synthesis at temperatures below 600°C resulted in the increased presence of multilayer graphene and amorphous carbon.

Those works have inspired us to explore novel experimental method by utilizing PECVD to decompose C_2H_2 on different bimetallic or alloy catalysts. Considering the much lower graphene growth temperature required for Ni surface than that for Cu surface, we use Ni as primary catalyst to further reduce the growth temperature. In the meantime, the theoretical simulation is performed to investigate the catalytic activities of different alloy surfaces. Both experimental and simulational results are demonstrated in this paper.

In this study, density functional theory is employed to calculate the total energy of decomposition of C_2H_2 on (100) catalysts surface of $Ni_{1-x-y}Au_xCu_y$ alloy (here x is the mol fraction of Au, and y is the mol fraction of Cu), which is the first time to use this type of ternary alloy catalyst for graphene formation on silicon dioxide (SiO₂) by PECVD. To investigate the simulation results, the reaction energies (E_R) to decompose the C-H bonds and $C \equiv C$ bonds of C_2H_2 on different catalysts surfaces are compared, and a differential energy (E_D) is proposed to scale the difficulties to decompose C-H bonds or $C \equiv C$ bonds and the modulation effects. The larger E_D is, the easier to grow monolayer graphene at reduced temperature.

The simulations have revealed that by employing Ni catalyst alloys, in which small mol fractions of Au $(x \approx 0.0313)$ and Cu $(y \approx 0.0313)$ can be varied, E_D s are all positive, thus it is possible to tune the reaction energy with respect to the decomposition of C-H bonds and C=C bonds of C_2H_2 , meanwhile, modulate the catalytic activity to favor the monolayer growth of graphene. By such a modulation and optimization, it is expected that the growth of graphene with controlled layer formation and improved defect density at reduced growth temperature can be achieved. Using this strategy, we have successfully grown uniform monolayer graphene on SiO₂ substrate at 500 °C by PECVD with C_2H_2 precursor and Ni alloy catalysts with 1 wt% Au and 1 wt% Cu.

2. Methods

2.1. Model and simulation

First principle simulation was carried out with ABINIT software [28]. In the calculation of total energies, the k-point mesh is set as $3 \times 3 \times 3$, with a tolerance on the difference of total Hartree energy of 1.0E-5, and the maximal number of SCF cycles of 100.

The Ni_{1-x-y}Au_xCu_y (100) surface is simulated with a four-layer-thick periodic slab model with a ~10Å vacuum, which is composed of $4 \times 4 \times 4$ periodic unit cells, as shown in figure 1(a). The C₂H₂ molecule is horizontally mounted on the surface at 0.55, the optimized relative height of model.

Together with C_2H_2 molecule above the supercell, this model consists of 68 atoms, making it possible to investigate the difference of $Ni_{1-x-y}Au_xCu_y$ alloy effects with approximately 1% resolution of mol fraction x and/or y. The (100) surface is employed because the Ni(100) surface was found to be more active than the Ni(111) surface, but with only a slight difference in the decomposition on different crystal orientations [16]. Ni_{1-x-y}Au_xCu_y alloys are simulated by substituting the first neighbor atoms 1–2, the second neighbor atoms 3–4, and/or the third neighbor atoms 5–8 with Au or Cu atoms on the top/second layer of slab model. For convenience of further discussion in the following text, here we simply denote the surface of pure Ni (100) surface (i.e. x = y = 0 in $Ni_{1-x-y}Au_xCu_y$) as Ni, and those surface of alloys with one or two atoms of Au and/or Cu in the slab model as 1Au, 2Au, 1Cu, 2Cu, 1Au1Cu, 2Au2Cu, respectively.

The decomposition of a C_2H_2 molecule was simulated by four steps. First it initiates from the conversion of the C_2H_2 in the gas state into the adsorption state on the Ni alloy surface, and we assign it as C_2H_2 or step 1, as shown in figure 1(b). After overcoming an energy barrier, one H atom is decomposed from C_2H_2 , moving to the

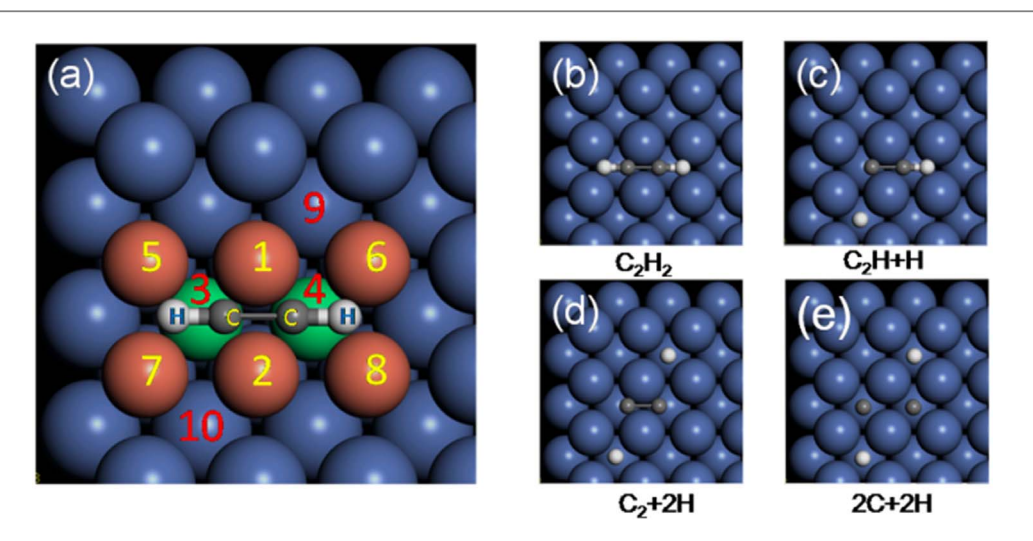


Figure 1. Top view of $4 \times 4 \times 4$ supercell model in four steps of decomposition. (a) Atoms 1, 2, 5, 6, 7, 8 are in the top layer, and atoms 3, 4, 9, 10 are in the second layer. The C_2H_2 molecule is horizontally mounted above the link of atoms 3 and 4. For pure Ni surface, atoms 1 to 8 are all Ni, and the alloy surface was realized by substituting some of them with Au or Cu atoms. (b) The C_2H_2 is not decomposed in step 1. (c) One H atom is decomposed to the top of atom 10 in step 2. (d) Another H atom is decomposed to the top of atom 9 in step 3. (e) Finally, the $C \equiv C$ bond is decomposed, demonstrated by moving the two carbon atoms to the top of atoms 3 and 4.

top of atom 10, as shown in figure 2(c). Hence C_2H_2 is transformed into the product of $C_2H + H$, assigned as step 2. Then the second H atom is decomposed, moving to the top of atom 9, resulting in the product of $C_2 + 2H$, assigned as step 3, as shown in figure 1(d). Finally, the $C \equiv C$ bond is decomposed, and $C_2 + 2H$ is transformed into 2C + 2H, with two carbon and two H atoms separated on the surface, assigned as step 4, as shown in figure 1(e).

2.2. Synthesis and measurements

A custom PECVD system equipped with remote inductively coupled plasma generation capabilities was used. Catalysts were deposited via magnetron sputtering for Ni and Cu and electron beam evaporation for Au in a Kurt J. Lesker Axxis PVD system. 50 nm catalysts were deposited on Si/SiO $_2$ wafers at 1 wt% Au, 2 wt%Cu, or 1 wt% Au together with 1 wt% Cu, with the remainder of the catalyst as Ni. Graphene synthesis was performed within the PECVD at a reaction temperature of 500 °C for 30s with a 10W inductively coupled plasma and 0.1 sccm flow rate of C_2H_2 at a chamber pressure of 4×10^{-6} torr. After the synthesis, the catalyst was etched away and graphene was transferred to a new SiO $_2$ substrate for Raman inspection in a Horiba Jobin Yvon Hr 800 spectrometer with a 532 nm excitation laser.

3. Result and discussion

3.1. Total energies at different decomposition steps, $E_T(i, j)$

Considering the effects of adsorption of C_2H_2 in relation to its decomposition, we calculated the total energies of the model in four steps denoted above. We denote the total energy of a certain surface by $E_T(i,j)$, where i is the type of catalyst surface, and j is the decomposition step. Since we are mainly concerned with the difference of the total energy between different steps for each surface, we then align $E_T(i,j) = E_T(i,j) \cdot E_T(i,1)$ to ensure $E_T(i,1) = 0$.

The simulation of decomposition of C_2H_2 on pure Ni surface was first considered since it is a common catalyst choice for the growth on Si/SiO_2 substrate at reduced temperatures. In step 1, the adsorption energy of the C_2H_2 can be calculated as the difference of the total energy (E_T) before and after the C_2H_2 is absorbed, [24,25] i.e., the adsorption energy (E_A) of C_2H_2 on Ni slabs is given by $E_A(C_2H_2) = E_T(C_2H_2/Ni_{slab}) - E_T(C_2H_2) - E_T(Ni_{slab})$. Since $E_T(C_2H_2)$ and $E_T(Ni_{slab})$ are both subtracted during the alignment, the aligned total energy E_T can be directly associated with the adsorption energy E_A . After the alignment, the total energy $E_T(Ni,1)$ is zero eV, then the $E_T(Ni,2)$ is 2.8022 eV after the first H atom is decomposed in step $E_T(Ni,3)$ is increased to $E_T(Ni,3)$ eV when the $E_T(Ni,3)$ is increased to $E_T(Ni,3)$ is further increased to $E_T(Ni,3)$ eV when the $E_T(Ni,3)$ is finally decomposed in step $E_T(Ni,3)$ is further increased to $E_T(Ni,3)$ eV when the $E_T(Ni,3)$ is finally decomposed in step $E_T(Ni,3)$ is further increased to $E_T(Ni,3)$ eV when the $E_T(Ni,3)$ is finally decomposed in step $E_T(Ni,3)$ is further increased to $E_T(Ni,3)$.

We then calculated $Ni_{1-x-y}Au_xCu_y$ alloy catalysts with different numbers of Au and Cu atoms in the periodic supercell model. The corresponding $E_T(i, j)$ for different surfaces are calculated and plotted in figure 2(a), one

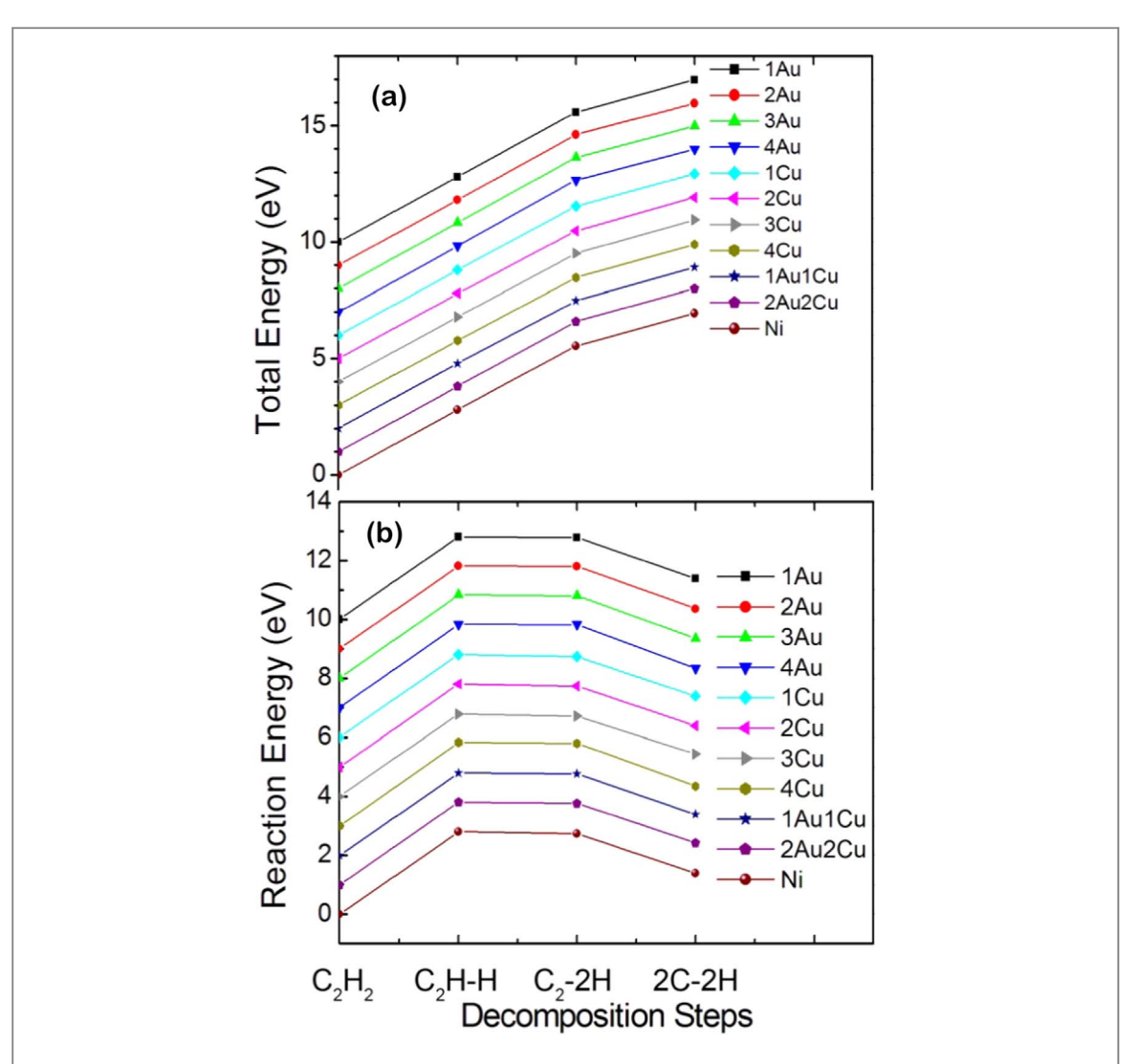


Figure 2. (a) $E_T(i,j)$ (eV), aligned total energies of different surfaces, by setting $E_T(i,1) = 0$ eV, plots are vertically translated for a better view. No obvious difference among them can be depicted. (b) $E_R(i,j)$, aligned reaction energies of each step for different surfaces. Setting $E_R(i,1) = 0$ eV, and plots are vertically translated as well. $E_R(i,j)$ are similar on most surface, close to that of Ni surface $E_R(Ni,j)$. This implies that the $C \equiv C$ bonds are much easier to decompose after the H atoms are decomposed.

curve for each surface, and they are vertically translated by 1 eV consecutively for each different surface, for observational convenience. The increasing trend of each plot looks very similar with no readily observed differences among them, where i stands for different catalyst surfaces, and j stands for different decomposition steps. For example $E_T(2Au, 4)$ is the total energy of C_2H_2 on 2Au surface in decomposition step 4. All $E_T(i, j)$ of the model in step 1 are aligned to zero eV, i.e., $E_T(i, 1) = 0$. The larger the total energy is, the more difficult the decomposition of C_2H_2 . $E_T(i, 4)$ for most surfaces are larger than that on Ni surface, except 1Cu and 2Cu surfaces. Thus the simulation reveals that it is more difficult to decompose C_2H_2 on those surfaces with larger $E_T(i, 4)$ than that of Ni surface, and consequently reduce the growth speed of graphene due to the lower decomposition activity.

3.2. Reaction energies at different decomposition steps, $E_R(i, j)$

In order to investigate the effects of different surfaces at different steps, we calculate the difference of total energy among consecutive steps for each surface, regarded as reaction energy and denoted as $E_R(i, j)$ by subtracting the total energies of previous steps, except in step 1, which is set to zero eV.

$$E_{R}(i, j) = \begin{cases} 0 \text{ (eV)} & j = 1\\ E_{T}(i, j) - E_{T}(i, j - 1) \text{ (eV)} & 2 \leq j \leq 4 \end{cases}$$
 (1)

Here i is the type of catalyst surface, and j is the decomposition step. For each surface i, $E_R(i, 2)$ is the reaction energy for dehydrogenation of the first H atom, $E_R(i, 3)$ is the reaction energy for dehydrogenation of the second H atom, and $E_R(i, 4)$ is the reaction energy of final decomposition of the C \equiv C bond of C_2H_2 , affecting the growth speed of graphene. For example, in the case of pure Ni surface, we set the reaction energy $E_R(N_i, 1) = 0$ eV, and

those of step 2, 3 and 4, namely, the reaction energy of first C-H bond $E_R(Ni, 2)$, the reaction energy of second C-H bond $E_R(Ni, 3)$, and the reaction energy of $C \equiv C$ bond $E_R(Ni, 4)$ are given by $E_T(Ni, 2) - E_T(Ni, 1)$, $E_T(Ni, 3) - E_T(Ni, 2)$, and $E_T(Ni, 4) - E_T(Ni, 3)$, respectively. The output of this procedure is plotted in figure 2(b). It can be seen that on all surfaces, the reaction energy of first C-H bond $E_R(i, 2)$ and the reaction energy of second C-H bond $E_R(i, 3)$ are similar, close to that of Ni surface, $E_R(Ni, 2) = 2.8022$ eV. This suggests that on most surfaces, the reaction energies of dehydrogenations are similar. Additionally, all the reaction energy of $C \equiv C$ bond $E_R(i, 4)$ are similar to that of Ni surface, $E_R(Ni, 4) = 1.39822$ eV, as shown in figure 2(b). This implies that the $C \equiv C$ bond is much easier to be decomposed after the H atoms were taken away. The reaction energies of each step associates with the complete decomposition of C_2H_2 , affecting the growth speed of graphene. The higher the reaction energy, the more difficult the corresponding decomposition step and the slower the graphene growth. Thus in order to modulate the growth speed and to achieve the monolayer growth, it is important to tune $E_R(i, 2)$, $E_R(i, 3)$ and $E_R(i, 4)$ altogether.

3.3. Differential energies at different decomposition steps, $E_D(i, j)$

To clearly show the difference of reaction energy on different surfaces of different steps, and scale the difficulty to decompose the C-H bonds and C \equiv C bond, we compare the reaction energy $E_R(i, j)$ of different surfaces with that of the Ni surface by $E_R(i, j)$ - $E_R(Ni, j)$, and denoted it as differential energy $E_D(i, j)$. The results of all differential energy $E_D(i, j)$ are plotted in figure 3.

$$E_{D}(i, j) = \begin{cases} 0 \text{ (eV)} & i = \text{Ni} \\ E_{R}(i, j) - E_{R}(Ni, j) \text{ (eV)} & i \neq \text{Ni, } 1 \leq j \leq 4 \end{cases}$$
 (2)

Similarly, i stands for different catalyst surfaces, and j stands for different decomposition steps. For example, $E_D(2Au, 4)$ is the difference between reaction energy of C_2H_2 on 2Au surface in decomposition step 4 and the reaction energy of C_2H_2 on pure Ni surface in step 4. If $E_D(i, j)$ is positive, the reaction energy on surface i at step j, $E_R(i, j)$ is larger than that on Ni surface. Vice versa, if $E_D(i, j)$ is negative, $E_R(i, j)$ is smaller than that on Ni surface.

In figure 3(a), it is shown that on NiAu surfaces, (i = 1Au, 2Au, 3Au, 4Au), the differential energies $E_D(i, 2)$ and $E_D(i, 3)$ are mostly positive while $E_D(i, 4)$ are negative. This means with the increase of Au atoms, $E_R(i, 2)$ and $E_R(i, 3)$, the reaction energies of dehydrogenations are larger than those on the Ni surfaces, but $E_R(i, 4)$, the reaction energy of $C \equiv C$ bond is smaller than that on the Ni surface. On the contrary, as shown in figure 3(b), on NiCu surfaces, (i = 1Cu, 2Cu, 3Cu, 4Cu), $E_D(i, 2)$ and $E_D(i, 3)$ are mostly negative while $E_D(i, 4)$ are mostly positive.

This means with the increase of Cu atoms, $E_R(i,2)$ and $E_R(i,3)$, the reaction energies of dehydrogenations are smaller than that on the Ni surface, but the reaction energy of $C \equiv C$ bond $E_R(i,4)$ is mostly larger than that on the Ni surface. On NiAuCu surfaces (i=1Au1Cu, 2Au2Cu), the modulated effects can be clearly observed in figure 3(c). The differential energies $E_D(i,2)$, $E_D(i,3)$ and $E_D(i,4)$ are mostly positive. This means their corresponding reaction energies $E_R(i,2)$, $E_R(i,3)$ and $E_R(i,4)$, especially on 2Au2Cu surface, all are larger than that on a Ni surface. This suggests that by employing $Ni_{1-x-y}Au_xCu_y$ catalyst, in which Ni as a primary catalyst, with small fraction of Au or together with $Cu(x \approx y \approx 0.0313)$, we can reduce the growth temperature, and meanwhile, reduce the carbon decomposition speed for monolayer growth, making it an effective, tunable growth condition.

As we mentioned above, when $i \neq Ni$, $E_D(i,j)$, the difference between reaction energy $E_R(i,j)$ and $E_R(Ni,j)$ show the difficulties to decompose C-H bonds or $C \equiv C$ bond on surface i. Compare to that on Ni surface, on NiAu surfaces, (i = 1Au, 2Au, 3Au, 4Au), since the overall total energies at step 4 $E_T(i,4)$ are larger than that on Ni surface $E_T(Ni,4)$, the adoption of NiAu alloy will consequently cause some difficulties for speedly decompostion of C_2H_2 , hence slightly reduce the growth speed. While on NiCu surfaces (i = 1Cu, 2Cu, 3Cu, 4Cu), since the overall total energies on NiCu surfaces at step 4 are mostly slightly larger than that on a Ni surface, the adoption of the NiCu alloy will also slightly reduce the growth speed, because the difficulty to decompose the $C \equiv C$ bonds increases. For the case on NiAuCu surface, since most differential energies $E_D(i,j)$ (i = 1Au1Cu, 2Au2Cu; j = 2, 3, 4) are positive, it means most of the reaction energies to decompose the C-H bond or $C \equiv C$ bond increase. The overall total energies at step 4, $E_T(i,j)$ (i = 1Au1Cu, 2Au2Cu; i = 1) are also higher than that on Ni surface. It will consequently increase the difficulty of $E_T(i,j)$ (i = 1Au1Cu, 2Au2Cu; i = 1Au1 are also higher than that on Ni surface. It will consequently increase the difficulty of $E_T(i,j)$ (i = 1Au1Cu, 2Au2Cu; i = 1Au1 are also higher than that on Ni surface. It will consequently increase the difficulty of $E_T(i,j)$ (i = 1Au1Cu, 2Au2Cu; i = 1Au1 are also higher than that on Ni surface. It will consequently increase the difficulty of $E_T(i,j)$ (i = 1Au1Cu, 2Au2Cu; i = 1Au1 are also higher than that on Ni surface. It will consequently increase the difficulty of $E_T(i,j)$ (i = 1Au1Cu, 2Au2Cu; i = 1Au1 are also higher than that on Ni surface. It will consequently increase the difficulty of $E_T(i,j)$ (i = 1Au1Cu, 2Au2Cu; i = 1Au1Cu

3.4. PECVD growth of graphene at 500 °C

To validate the calculation results, graphene has been grown by PECVD on various Ni and Ni alloy catalysts at 500°C, with Raman maps displayed in figure 4. Note these maps in figures 4(a)–(d) where the multilayer

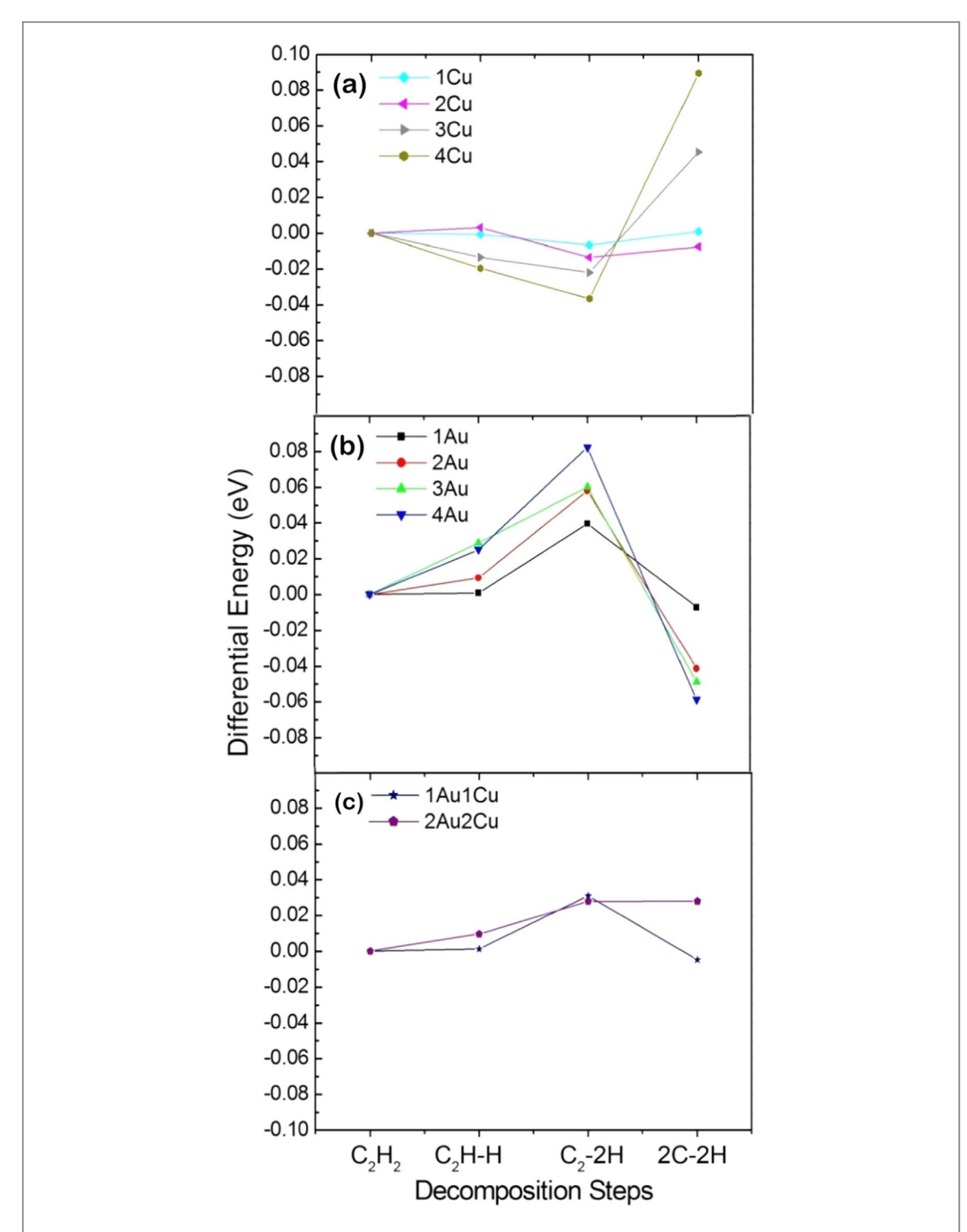


Figure 3. The differential energy $E_D(i, j)$, i.e., the differences of reaction energies $E_R(i, j)$ of each step for different surfaces, compared to that of C_2H_2 on Ni surface. The difference of reaction energies with the increasing of (a) Au on 1Au, 2Au, 3Au, 4Au surfaces, (b) Cu on 1Cu, 2Cu, 3Cu, and 4Cu surfaces, (c) both Au and Cu on 1Au1Cu and 2Au2Cu surfaces.

portions of the graphene film, with a Raman intensity ratio $I_{2D/G} \le 1$, appear black while the few layers or monolayer of graphene appear light orange and white, respectively.

Our experimental results indicate when synthesis is performed on a pure Ni catalyst, displayed in figure 4(a), multilayer graphene dominates the growth. This is consistent with our calculation that pure Ni's reaction energy is favorable for decomposition of the C_2H_2 precursor and a rapid growth resulting in multilayer production. For the addition of 1 wt% Au and 2 wt% Cu, the results are shown in figures 4(b) and (c) respectively. Note that a reduction of multilayer formation is obvious, although some multilayer islands still remain. Finally, the Ni alloy catalyst with 1 wt% Au and 1 wt% Cu was used and the result is shown in figure 4(d). Note that no multilayer portions of the film are observed suggesting that the majority of the graphene films are monolayer. This result is

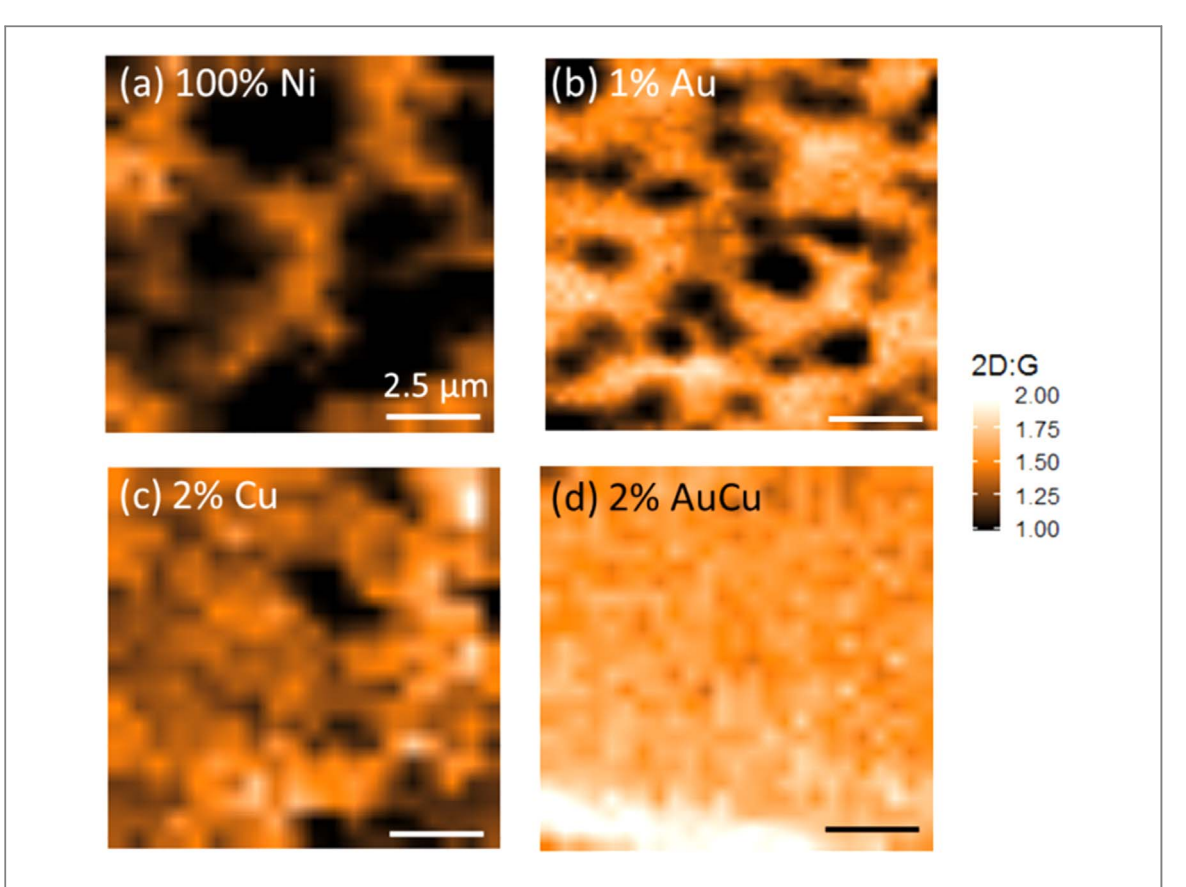


Figure 4. 10 μ m² Raman maps displaying $I_{2D/G}$ ratio for (a) Ni, (b) 1 wt% Au, (c) 2 wt% Cu and (d) 2 wt % AuCu surfaces. All scale bars are 2.5 μ m and multilayer portions of the film are indicated in black ($I_{2D/G} \le 1$). Significant portions of multilayer are observed on (a) the pure Ni catalyst while multilayer portions remain on both (b) NiAu and (c) NiCu catalysts. However, on (d) the NiAuCu catalyst, no multilayer portions of the film are observed.

consistent with our simulation in confirming that the catalytic activity of NiAuCu alloy has been tuned to enable the growth of uniform monolayer graphene..

3.5. Modulated effects of NiAuCu alloy

The total energy E_T , the reaction energy E_R and differential energy are related to the growth temperature and growth mode resulting in either monolayer or multilayer. The smaller the E_T , the lower the temperature required to achieve successful growth of graphene. Since most $E_T(i, j)$ before alignment are close to $E_T(Ni, j)$, we can grow the graphene at low temperature similar that on Ni surface. On the other hand, the larger reaction energies $E_R(i,j)$ (j=2,3 for C-H bonds, j=4 for C \equiv C bond), the larger $E_D(i,j)$, and the more difficult to decompose the C_2H_2 completely, thus the easier to achieve monolayer growth of graphene. The Raman $I_{2D/G}$ mapping of the samples in figure 4 shows that, for NiAu and NiCu surfaces, it is easier to achieve monolayer growth at 500 °C, so their reaction energies of C-H and/or C≡C bonds must be larger than the corresponding reaction energies on Ni surface, and their differential energies are positive. This is consistent with the simulation results in figure 3. For NiCu surface, the modulation effect to achieve the monolayer growth is mostly due to larger reaction energy of C \equiv C bond, $E_R(i, 4)$, and positive $E_D(i, 4)$. For NiAu surface, such effect is mostly due to larger dehydrogenation reaction energies $E_R(i, 2)$ and $E_R(i, 3)$, i.e., $E_D(i, 2)$ and $E_D(i, 3)$ are positive. For NiAuCu surface, the corresponding reaction energies $E_R(2Au2Cu, 3)$ and $E_R(2Au2Cu, 4)$ are larger than that on Ni surface, i.e., $E_D(2Au2Cu, 3)$ and $E_D(2Au2Cu, 4)$ are positive. Thus both the decomposition activity of C–H and C≡C bonds have been modulated lower, so the growth speed is greatly reduced, and the catalytic activity is controlled, making it possible to achieve monolayer growth at lower temperature. This is confirmed by the largest average I2D/G(AuCu) in figure 4. Therefore, our simulation and experiments of monolayer growth match very well and can provide support for further optimization in low temperature growth of large-scale, high quality graphene through an in-depth understanding the synergistic effects among growth parameters.

4. Conclusion

First principle simulations of different stages of decomposition of C_2H_2 on (100) catalysts surface of Ni, NiAu, NiCu and NiAuCu alloy were carried out. A differential energy is proposed to scale the difficulty to decompose the C–H bonds and C \equiv C bonds. For the NiAu surfaces, when the Au atoms increase, the differential energy of C–H bonds are positive, at the same time, the differential energy of decompose C \equiv C bond is negative. For the NiCu surfaces, when the Cu atoms increase, the differential energy of C–H bonds are negativewhile that of C \equiv C bond is positive. For NiAuCu alloy catalyst surfaces, where two Au and Cu atoms are in the 4 \times 4 \times 4 Ni supercell model, the differential energies of C–H bonds and C \equiv C bonds are positive, indicating an obvious modulated effect. The change of total energy, reaction energies, differential energy for different catalyst surfaces at different C_2H_2 decomposition stages provides a theoretical reference in optimizing the growth temperature and growth speed for the monolayer graphene growth. These results are consistent with our experiments in PECVD growth of graphene on Si/SiO₂ substrate with NiAuCu alloy catalyst at 500 °C.

Acknowledgments

The authors would like to acknowledge that this study is supported in part by the NSF award No. 1711994, Intel Corporation, and Oregon Metals Initiative.

ORCID iDs

```
Huahan Zhan https://orcid.org/0000-0002-3370-9193
Bin Jiang https://orcid.org/0000-0001-6210-1972
Otto Zietz https://orcid.org/0000-0002-5689-8070
Samuel Olson https://orcid.org/0000-0002-0264-2555
Jun Jiao https://orcid.org/0000-0002-3942-9598
```

References

- $[1]\ \ Novoselov\ K\ S,\ Falko\ V\ I,\ Colombo\ L,\ Gellert\ P\ R,\ Schwab\ M\ G\ and\ Kim\ K\ 2012\ \textit{Nature}\ 490\ 192$
- $[2] \ Castro\ Neto\ A\ H, Guinea\ F, Peres\ N\ M\ R, Novoselov\ K\ S\ and\ Geim\ A\ K\ 2009\ \textit{Review of Modern Physics}\ \textbf{81}\ 109$
- [3] Meric I, Han MY, Young AF, Ozyilmaz B, KimP and Shepard KL 2008 Nature Nano. 3 654
- [4] Georgakilas V, Otyepka M, Bourlinos AB, Chandra V, Kim N, Kemp KC, Hobza P, Zboril R and Kim KS 2012 Chem. Rev. 112 6156
- [5] Kim K S, Zhao Y, Jang H, Lee S Y, Kim J M, Kim K S, Ahn J-H, Kim P, Choi J-Y and Hong B H 2009 Nature 457 706
- [6] Li X et al 2009 Science 324 1312
- [7] Lampert L F, Caudillo R, Lindner T and Jiao J 2016 J. Phys. Chem. C 120 26498
- [8] Kim J, Masatou I, Koga Y, Tsugawa K, Hasegawa M and Iijima S 2011 Appl. Phys. Lett. 98 091502
- [9] Obraztsov A N, Obraztsova E A, Tyurnina A V and Zolotukhin A A 2007 Carbon 45 2017
- [10] Terasawa T and Saiki K 2012 Carbon 50 869
- [11] Chen S, Cai W, Piner R D, Suk J W, Wu Y, Ren Y, Kang J and Ruoff R S 2011 Nano Lett. 11 3519
- [12] Seah C-M, Chai S P and Mohamed A R 2014 Carbon 70 1
- [13] Greeley J and Mavrikakis M 2004 Nature Mat. 3 810
- [14] Dai B, Fu L, Zou Z, Wang M, Xu H, Wang S and Liu Z 2011 Nature Comm. 2 522
- [15] Woo Y S et al 2013 Carbon 64 315
- [16] Wang X, Yuan Q, Li J and Ding F 2017 Nanoscale 9 11584
- [17] Liu W, Li H, Xu C, Khatami Y and Banerjee K 2011 Carbon 49 4122
- [18] Besenbacher F, Chorkendorff I, Clausen B S, Hammer B, Molenbroek A M, Nørskov J K and Stensgaard I 1998 Science 279 1913
- [19] Li X, Cai W, Colombo L and Ruoff R S 2009 Nano Lett. 9 4268
- [20] Li X et al 2010 Nano Lett. 10 4328
- [21] WuY et al 2012 ACS Nano 6 7731
- [22] Sutter PW, Flege J and Sutter EA 2008 Nature Mat. 7 406
- [23] Meca E, Lowengrub J, Kim H, Mattevi C and Shenoy V B 2013 Nano Lett. 13 5692
- [24] Nie S, Bartelt N C, Wofford J M, Dubon O D, McCarty K F and Thurmer K 2012 Phys. Rev. B: Condens. Matter. 85 205406
- [25] Zhang W, Wu P, Li Z and Yang J 2011 J. Phys. Chem. C 115 17782
- [26] Gao M, Pan Y, Huang L, Hu H, Zhang L Z, Guo H M, Du S X and Gao H-J 2011 Appl. Phys. Lett. 98 033101
- [27] Liu X, Fu L, Liu N, Gao T, Zhang Y, Liao L and Liu Z 2011 J. Phys. Chem. C 115 11976
- [28] Gonze X et al 2016 Comput. Phys. Commun 205 106-31